

# Activating transcription factor 3 inhibits angiotensin II-induced cardiomyocyte viability and fibrosis by activating the transcription of cysteine-rich angiogenic protein 61

YU ZHANG<sup>1</sup>, HEMING WU<sup>2</sup>, HONGHUI LUO<sup>1</sup>, YIQUN LUO<sup>1</sup> and CONG HUANG<sup>1</sup>

<sup>1</sup>Department of General Practice; <sup>2</sup>Central Laboratory, Meizhou People's Hospital, Meizhou, Guangdong 514031, P.R. China

Received February 14, 2022; Accepted August 22, 2022

DOI: 10.3892/mmr.2022.12852

**Abstract.** Depletion of activating transcription factor 3 (ATF3) expression has previously been reported to promote hypertrophy, dysfunction and fibrosis in stress overload-induced hearts; however, the mechanism involved remains poorly understood. In the present study, the mechanism underlying the activation of cysteine-rich angiogenic protein 61 (Cyr61) by ATF3 in hyperproliferative and fibrotic human cardiac fibroblasts (HCFs), induced by angiotensin II (Ang II), was evaluated. The mRNA and protein expression levels of ATF3 and Cyr61 were assessed using reverse transcription-quantitative PCR and western blotting, respectively. The Cell Counting Kit-8 assay was used to assess cell viability. Cell migration was assessed using the wound healing assay and western blotting, whereas the extent of cell fibrosis was evaluated using immunofluorescence staining and western blotting. The binding site of ATF3 to the Cyr61 promoter was predicted using the JASPAR database, and verified using luciferase reporter and chromatin immunoprecipitation assays. The results demonstrated that the mRNA and protein expression levels of ATF3 were significantly upregulated in Ang II-induced HCFs. Overexpression of ATF3 significantly inhibited the Ang II-induced viability, migration and fibrosis of HCFs, whereas ATF3 knockdown mediated significant opposing effects. Mechanistically, ATF3 was demonstrated to transcriptionally activate Cyr61. Cyr61 silencing was subsequently revealed to reverse the effects of ATF3 overexpression on HCFs potentially via regulation of the TGF- $\beta$ /Smad signaling pathway. The results of the present study suggested that ATF3 could suppress HCF viability and fibrosis via the TGF- $\beta$ /Smad signaling pathway by activating the transcription of Cyr61.

## Introduction

Cardiac hypertrophy is a compensatory reaction to myocardial stress overload, and is characterized by increased protein synthesis, myocardial cell volume enlargement and mesenchymal component alterations (1-3). Cardiac hypertrophy is an independent risk factor for cardiovascular disease morbidity and mortality (4). Numerous parameters have been reported to contribute to this disease, including neurohormonal factors, mechanical factors, endocrine factors, sympathetic nervous system activity and nitric oxide production (2,5). At present, treatment of cardiac hypertrophy mainly involves the application of angiotensin-converting enzyme inhibitors, angiotensin II (Ang II) receptor blockers, calcium channel blockers,  $\beta$ -receptor blockers and diuretics (6-8). However, the therapeutic effects mediated by these strategies remain unsatisfactory. Therefore, there is a demand for novel therapeutic options for cardiac hypertrophy.

Activating transcription factor (ATF) 3 is a member of the ATF/cAMP-responsive element-binding protein family of transcription factors (9). ATF3 is a stress response protein that is expressed at low levels in quiescent cells but is increased under various stress stimuli, such as injury and toxin exposure, and has been reported to facilitate the pathological processes of various diseases, including hepatic ischemia-reperfusion, liver fibrosis and acute lung injury (10-12). For example, Chen *et al* (13) reported that acute hypoxia promoted the activation of ATF3, which could serve important roles in the cellular response to stress. It has also been reported that ATF3 can bidirectionally regulate the transcription of target genes (14,15). Furthermore, ATF3 may regulate the inflammatory response, apoptosis and autophagy by modulating the binding sites of transcription factors, such as transcriptional activating protein-1, NF- $\kappa$ B and p53 (16,17). Previous studies have reported that ATF3 serves an important role in the occurrence and development of various forms of cardiovascular diseases, such as myocardial ischemia-reperfusion injury, myocardial hypertrophy and heart failure (18-20). As such, ATF3 deficiency has been reported to promote pressure overload-induced cardiac hypertrophy, dysfunction and fibrosis (21). However, the mechanism underlying the regulatory effects of ATF3 during myocardial hypertrophy remain elusive.

In the present study, the role and mechanism of action of ATF3 in cardiac hypertrophy were assessed. Ang II treatment

**Correspondence to:** Dr Yu Zhang, Department of General Practice, Meizhou People's Hospital, 63 Huangtang Road, Meizhou, Guangdong 514031, P.R. China  
E-mail: zyzhangyu1@126.com

**Key words:** activating transcription factor 3, cardiac hypertrophy, angiotensin II, proliferation, fibrosis, cysteine-rich angiogenic protein 61

was used to establish an *in vitro* model of cardiac hypertrophy before the effects of ATF3 on Ang II-induced cardiomyocytes, in addition to the association between ATF3 and cysteine-rich angiogenic protein 61 (Cyr61), were assessed.

## Materials and methods

**Cell culture and treatment.** Primary human cardiac fibroblasts (HCFs; cat. no. 6320) were purchased from ScienCell Research Laboratories, Inc. The cells were cultured in DMEM (Gibco; Thermo Fisher Scientific, Inc.) supplemented with 10% FBS (Gibco; Thermo Fisher Scientific, Inc.), 100  $\mu$ g/ml streptomycin and 100 U/ml penicillin in humidified conditions with 5% CO<sub>2</sub> at 37°C. Cellular hypertrophy of HCFs was induced using 1  $\mu$ mol/l Ang II (Sigma-Aldrich; Merck KGaA) at 37°C for 24 h. The concentration of Ang II was outside the range that reflects the *in vivo* situation and has been used in a similar manner in previous publications (22–24).

**Cell transfection.** The ATF3-specific pcDNA3.1 overexpression vector (Oe-ATF3) and empty plasmid (as the corresponding control Oe-NC), the specific small interfering RNAs (siRNAs) targeting ATF3 (si-ATF3-1, 5'-CGUGCAGUAUCUCAA GAUAAU-3'; si-ATF3-2, 5'-GGUUGUGCUUUCUAGCAA AUA-3') and Cyr61 (si-Cyr61-1, 5'-GAUUAGUUGGACAGU UAAAG-3'; si-Cyr61-2, 5'-AGAUUAGUUGGACAGUUU AAA-3'), and the non-targeting corresponding control (si-NC, 5'-UUCUCCGAACGUGUCACGU-3') were all purchased from Shanghai GenePharma Co., Ltd. These vectors (4  $\mu$ g) and siRNAs (100 nM) were transfected into HCFs (1 $\times$ 10<sup>5</sup> cells/well) seeded into 12-well plates using Lipofectamine<sup>®</sup> 2000 reagent (Invitrogen; Thermo Fisher Scientific, Inc.) at 37°C for 5 h according to the manufacturer's protocol. Next, the cells were incubated in DMEM supplemented with 10% FBS at 37°C for 48 h. At 48 h post-transfection, cells were collected for subsequent experiments.

**Cell Counting Kit-8 (CCK-8) assay.** HCFs, with or without transfection, were seeded into 96-well plates at a density of 1 $\times$ 10<sup>3</sup> cells/well and cultured in DMEM with 10% FBS, followed by treatment with Ang II. After 24 h, 10  $\mu$ l CCK-8 solution (Beijing Solarbio Science & Technology Co., Ltd.) was added into each well before incubation for a further 2 h. The absorbance value was detected at a wavelength of 450 nm using a microplate reader.

**Reverse transcription-quantitative PCR (RT-qPCR).** After treatment, total RNA was extracted from HCFs using TRIzol<sup>®</sup> (Invitrogen; Thermo Fisher Scientific, Inc.) according to the manufacturer's protocol. A NanoDrop<sup>®</sup> 3000 spectrophotometer (Thermo Fisher Scientific, Inc.) was used to confirm the quality and quantity of total RNA. RT of first-strand cDNA was performed using the PrimeScript<sup>™</sup> RT Master Mix (Perfect Real Time) kit (Takara Bio, Inc.) according to the manufacturer's protocol. Amplification of the cDNA was performed by qPCR using the TB Green Premix Ex Taq II kit (Takara Bio, Inc.). The PCR program was 95°C for 3 min, followed by 35 cycles of denaturation at 95°C for 30 sec, annealing at 60°C for 30 sec and extension at 72°C for 1 min. A final extension step at 72°C for 7 min was performed for each PCR assay.

The primer sequences used were as follows: ATF3 forward (F), 5'-AGCACCTTGCCCCAAAATCA-3' and reverse (R), 5'-AGGGCGTCAGGTTAGCAAAA-3'; Cyr61 F, 5'-AGC GTTCCCTTCTACAGGC-3' and R, 5'-TTCTCCAATCGT GGCTGCAT-3'; and GAPDH F, 5'-GGGAAACTGTGGCGT GAT-3' and R, 5'-GAGTGGGTGTCGCTGTTGA-3'. The relative mRNA expression levels were normalized to those of GAPDH using the 2<sup>- $\Delta\Delta C_q$</sup>  method (25).

**Wound healing assay.** The migratory capacity of cells was assessed using the wound healing assay. Transfected or untransfected cells were seeded into six-well plates, and cultured to 90% confluence following treatment with 1  $\mu$ mol/l Ang II (Sigma-Aldrich; Merck KGaA). The cell monolayers were then wounded using a 200- $\mu$ l pipette tip and washed three times with serum-free medium. After 24 h of incubation in serum-free medium at 37°C, images were captured using a light microscope (Leica Microsystems, Inc.) and the migration rate was calculated using the following formula: (scratch width at 0 h-scratch width at 48 h)/scratch width at 0 h. The wound closure area of the migrating monolayer of cells was quantified using ImageJ software (version 1.49; National Institutes of Health).

**Immunofluorescence staining.** Immunofluorescence staining was used for the assessment of the expression of  $\alpha$ -smooth muscle actin ( $\alpha$ -SMA) in HCFs. Cells were fixed with 4% paraformaldehyde at 37°C for 30 min, blocked with 5% bovine serum albumin (Beijing Solarbio Science & Technology Co., Ltd.) at 37°C for 30 min and incubated with anti- $\alpha$ -SMA antibodies (1:1,000; cat. no. 19245; Cell Signaling Technology) overnight at 4°C. Subsequently, Alexa Fluor<sup>®</sup> 488-conjugated secondary antibodies (1:400; cat. no. ab150077; Abcam) were added for 1 h at room temperature. The nuclei were stained using 5  $\mu$ g/ml DAPI solution for 5 min at room temperature. The cells were subsequently observed and images were captured using a fluorescence microscope (Olympus Corporation).

**Luciferase reporter assay.** The 3'UTR fragments of the human Cyr61 promoter were predicted using the JASPAR database 2022 (<https://jaspar.genereg.net>). Wild-type (WT) and corresponding mutant (Mut) fragments of the Cyr61 promoter covering the predicted DR1 (direct repeat motif with a single nucleotide spacer) sites were cloned into the firefly luciferase reporter plasmid pGL3-basic vector (Promega Corporation). Luciferase activity was then detected using a Dual-Luciferase Reporter Assay Kit (Promega Corporation) 48 h after transfection of WT/MUT plasmids and OE-ATF3/OE-NC into HCFs using the Lipofectamine 2000 transfection reagent. Firefly luciferase activity was normalized against that of the *Renilla* construct and the relative luciferase activity in untreated cells was designated as 1.

**Chromatin immunoprecipitation (ChIP) assay.** ChIP assays were performed using the EZ ChIP<sup>™</sup> Kit (MilliporeSigma). The cells were first cross-linked with 1% formaldehyde for 10 min at 37°C and quenched with 2.5 M glycine for 5 min at room temperature to a final concentration of 125  $\mu$ M. The fixed cells were washed twice with phosphate-buffered saline and were lysed using a lysis buffer [0.1% sodium dodecyl

sulfate (SDS), 0.5% Triton X-100, 20 mM Tris-HCl, pH 8.1] that contained 150 mM NaCl and a protease inhibitor. The lysed cells were subsequently subjected to sonication in ice water. The resulting sonicated fragments were within the size range of 200-1,000 bp. Following sonication, the samples were centrifuged at  $13,000 \times g$  for 10 min at 4°C, and 100  $\mu$ l of supernatant was pre-absorbed by 30  $\mu$ l protein G magnetic beads (Thermo Fisher Scientific, Inc.) conjugated to ATF3 antibodies (2  $\mu$ g; cat. no. ab254268; 1:30; Abcam) and IgG (as the NC; cat. no. ab172730; 1:50; Abcam). The immunoprecipitated complex was centrifuged ( $5,000 \times g$  for 1 min at 4°C) and washed with low salt, high salt, LiCl and TE buffers in the kit according to the manufacturer's protocols. The complex was eluted from the antibody using a solution of 1% SDS, 0.1 mol/l NaHCO<sub>3</sub> and 200 mmol/l NaCl. The resultant complex was incubated in 5 M NaCl and 20 mg/ml proteinase K solution (Cell Signaling Technology, Inc.) at 65°C for 2 h for the reversal of crosslinking. After crosslink reversal, precipitated DNA was analyzed by PCR for the 3'UTR fragments of the Cyr61 promoter. The input DNA and immunoprecipitated DNA underwent qPCR using SYBR® Green Real-time PCR Master Mix (Toyobo Life Science). The primer sequences for PCR were as follows: ATF3 forward, 5'-AGCACCTTGCCCCAAAATCA-3' and reverse, 5'-AGGGCGTCAGGTTAGCAAAA-3'; Cyr61 forward, 5'-AGCGTTTCCCTTCTACAGGC-3' and reverse, 5'-TTCTCCAATCGTGGCTGCAT-3'; and GAPDH forward, 5'-GGGAACTGTGGCGTGAT-3' and reverse, 5'-GAGTGGGTGTCGCTGTTGA-3'. The PCR program was 95°C for 3 min, followed by 35 cycles of denaturation at 95°C for 30 sec, annealing at 60°C for 30 sec and extension at 72°C for 1 min. A final extension step was applied at 72°C for 7 min. The data obtained were normalized to those obtained from the qPCR of the DNA precipitated by the IgG antibody. The relative mRNA expression levels were normalized to those of GAPDH using the  $2^{-\Delta\Delta C_q}$  method (25).

**Western blotting.** Total protein was extracted from treated or untreated HCFs using RIPA buffer (Beyotime Institute of Biotechnology) and quantified using the bicinchoninic acid method (Thermo Fisher Scientific, Inc.). Protein samples (40  $\mu$ g/lane) were then separated by SDS-PAGE on 10% gels and transferred onto PVDF membranes. The membranes, which were blocked with 5% skimmed fat milk overnight at 4°C, were incubated with the following primary antibodies overnight at 4°C: ATF3 (cat. no. ab254268; 1:1,000; Abcam), MMP-1 (cat. no. ab134184; 1:1,000; Abcam), MMP-2 (cat. no. ab92536; 1:1,000; Abcam), connective tissue growth factor (CTGF; cat. no. ab209780; 1:1,000; Abcam), fibronectin (cat. no. ab268020; 1:1,000; Abcam), collagen I (cat. no. ab138492; 1:1,000; Abcam), collagen III (cat. no. ab184993; 1:1,000; Abcam), Cyr61 (cat. no. ab230947; 1:1,000; Abcam), TGF- $\beta$  (cat. no. ab215715; 1:1,000; Abcam), phosphorylated (p)-Smad2 (cat. no. ab280888; 1:1,000; Abcam), p-Smad3 (cat. no. ab52903; 1:2,000; Abcam), Smad2 (cat. no. ab40855; 1:2,000; Abcam), Smad3 (cat. no. ab40854; 1:1,000; Abcam) and GAPDH (cat. no. ab9485; 1:2,500; Abcam). Membranes were washed with TBST (0.1% Tween-20) and incubated with HRP-conjugated secondary antibodies (cat. no. #7074; 1:3,000; Cell Signaling Technology, Inc.) for 1 h at room temperature. The immunoreactive protein bands were visualized using an

Amersham ECL Western Blotting Detection Reagent (Cytiva) and semi-quantified by densitometry (Quantity One® version 4.5.0; Bio-Rad Laboratories, Inc.).

**Statistical analysis.** All experiments were repeated three times independently. The data were analyzed using SPSS 17.0 software (SPSS, Inc.) and are presented as the mean  $\pm$  SD. Unpaired Student's t-test was used for comparisons between two groups. Differences among multiple groups were analyzed using one-way ANOVA with the Bonferroni multiple comparison post hoc test.  $P < 0.05$  was considered to indicate a statistically significant difference.

## Results

**ATF3 is highly expressed in Ang II-induced HCFs.** An *in vitro* cardiac hypertrophy model was established by stimulating HCFs with 1  $\mu$ mol/l Ang II. The results of RT-qPCR and western blotting demonstrated that the mRNA and protein expression levels of ATF3 were significantly upregulated in Ang II-induced HCFs compared with those in the untreated cells (Fig. 1A and B). To assess the role of ATF3 in cardiac hypertrophy, ATF3 expression was knocked down or ATF3 was overexpressed in HCFs. The transfection efficiency was assessed using RT-qPCR and western blotting. Oe-ATF3 transfection significantly increased the mRNA and protein expression levels of ATF3, whereas si-ATF3-1/2 transfection significantly reduced ATF3 mRNA and protein expression, compared with those in the negative control groups (Fig. 1C and D). Since si-ATF3-1 exhibited superior transfection efficiency, this siRNA was chosen for subsequent experiments and is referred to as si-ATF3 thereafter.

**Overexpression of ATF3 suppresses Ang II-induced viability, migration and fibrosis in HCFs.** The effect of ATF3 overexpression on Ang II-induced HCFs was assessed. Ang II treatment significantly enhanced HCF viability compared with that in the control group; however, transfection with Oe-ATF3 subsequently reversed this effect (Fig. 2A). Furthermore, wound healing assays demonstrated that treatment of HCFs with Ang II significantly increased the migratory rate compared with that in the control group in a manner that was reversed by ATF3 overexpression (Fig. 2B). Additionally, the protein expression levels of MMP-1 and MMP-2 were significantly increased following Ang II treatment compared with those in the control group; however, this effect was also reversed by transfection with Oe-ATF3 (Fig. 2C). Fibrosis was assessed using immunofluorescence staining and western blotting. Ang II treatment markedly increased the protein expression levels of  $\alpha$ -SMA compared with those in the control group, whereas the overexpression of ATF3 reversed this increase in  $\alpha$ -SMA expression (Fig. 2D). Marked increases in the protein expression levels of CTGF, fibronectin, collagen I and collagen III were also observed after the HCFs were treated with Ang II compared with those in the control group (Fig. 2E). However, ATF3 overexpression reversed the effects of Ang II on the protein expression levels of the aforementioned proteins in HCFs (Fig. 2E).

**Knockdown of ATF3 expression aggravates Ang II-induced viability, migration and fibrosis of HCFs.** To evaluate the role of



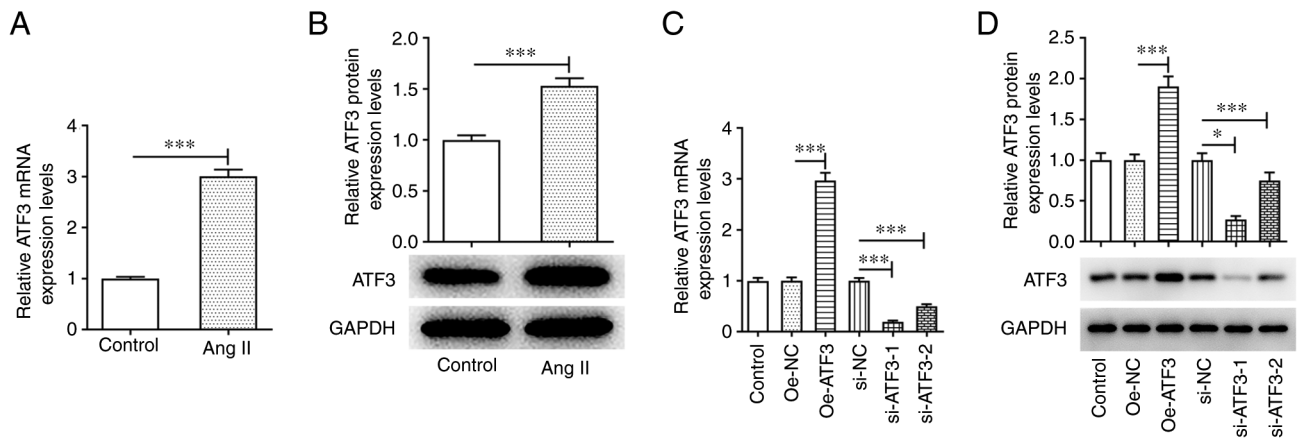


Figure 1. ATF3 is upregulated in Ang II-induced cardiac fibroblasts. (A) mRNA and (B) protein expression levels of ATF3 were assessed after treatment with Ang II by RT-qPCR and western blotting, respectively. (C) mRNA and (D) protein expression levels of ATF3 were assessed after transfection with different plasmids by RT-qPCR and western blotting, respectively. Data are presented as the mean  $\pm$  SD. \* $P$ <0.05, \*\*\* $P$ <0.001. ATF3, activating transcription factor 3; Ang II, angiotensin II; Oe, overexpression; NC, negative control; si, small interfering RNA; RT-qPCR, reverse transcription-quantitative PCR.

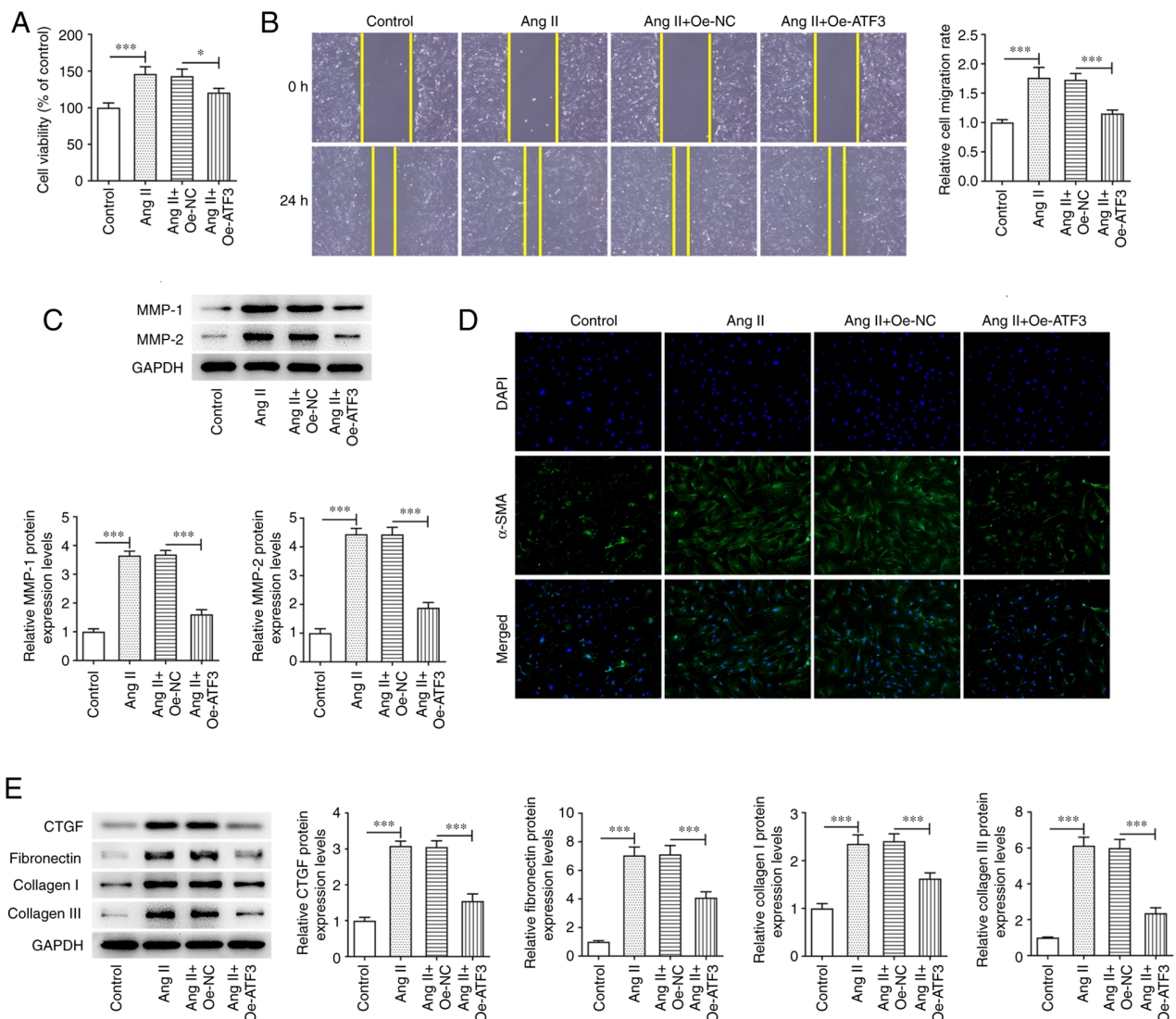


Figure 2. Overexpression of ATF3 inhibits Ang II-induced viability, migration and fibrosis in human cardiac fibroblasts. (A) Cell viability was evaluated using a Cell Counting Kit-8 assay. (B) Cell migration was assessed using the wound healing assay (magnification,  $\times 100$ ). (C) Protein expression levels of MMP-1 and MMP-2 were semi-quantified using western blotting. (D) Immunofluorescence staining was performed to assess the protein expression levels of  $\alpha$ -SMA (magnification,  $\times 200$ ). (E) Protein expression levels of CTGF, fibronectin, collagen I and collagen III were semi-quantified using western blotting. Data are presented as the mean  $\pm$  SD. \* $P$ <0.05, \*\*\* $P$ <0.001. ATF3, activating transcription factor 3; Ang II, angiotensin II;  $\alpha$ -SMA,  $\alpha$ -smooth muscle actin; CTGF, connective tissue growth factor; Oe, overexpression; NC, negative control.



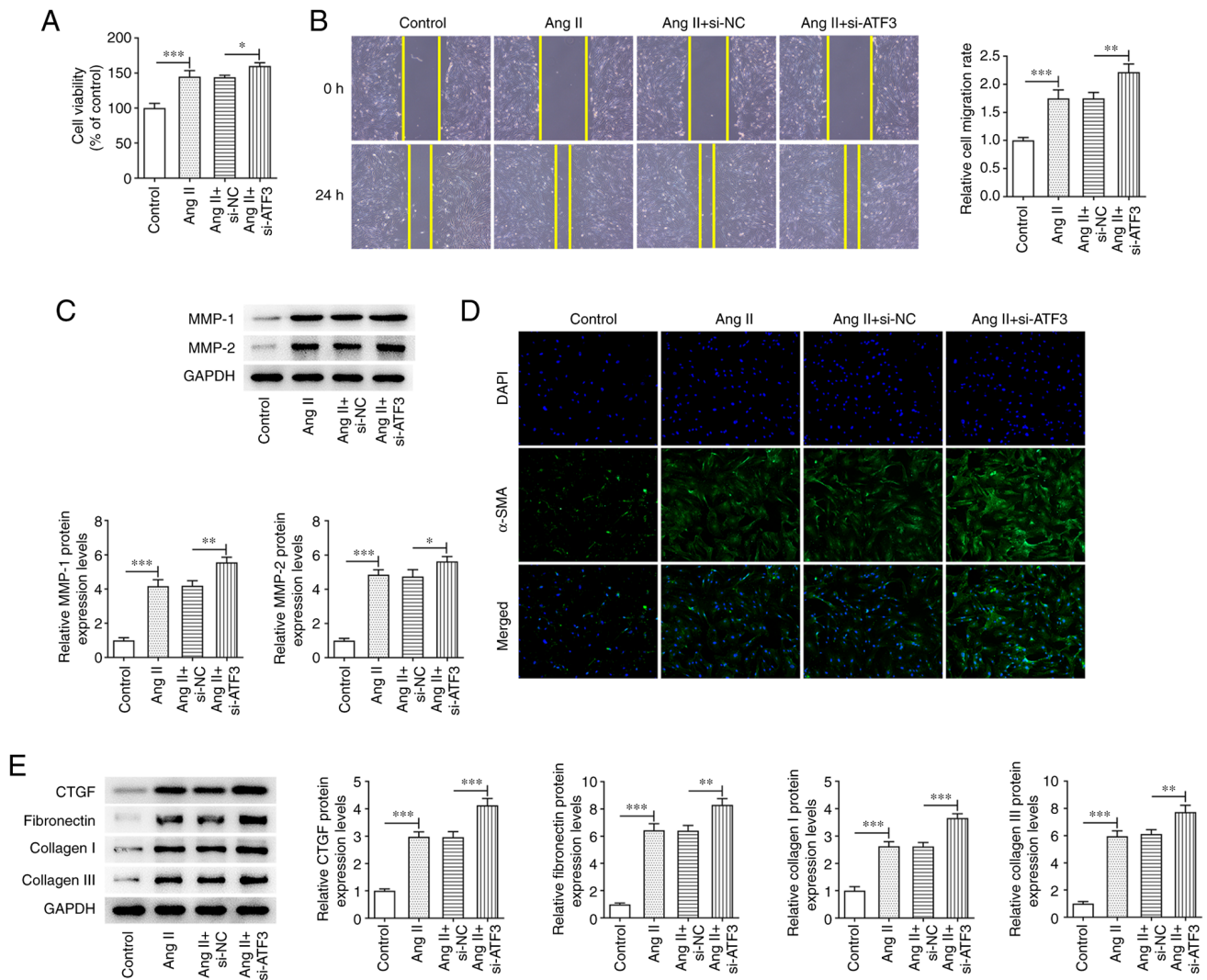


Figure 3. Knockdown of ATF3 promotes Ang II-induced viability, migration and fibrosis of cardiac fibroblasts. (A) Cell viability was evaluated using a Cell Counting Kit-8 assay. (B) Cell migration was evaluated using the wound healing assay (magnification, x100). (C) Protein expression levels of MMP-1 and MMP-2 were semi-quantified using western blotting. (D) Immunofluorescence staining was performed to assess the protein expression levels of  $\alpha$ -SMA (magnification, x200). (E) Protein expression levels of CTGF, fibronectin, collagen I and collagen III were semi-quantified using western blotting. Data are presented as the mean  $\pm$  SD. \* $P$ <0.05, \*\* $P$ <0.01, \*\*\* $P$ <0.001. ATF3, activating transcription factor 3; Ang II, angiotensin II;  $\alpha$ -SMA,  $\alpha$ -smooth muscle actin; CTGF, connective tissue growth factor; si, small interfering RNA; NC, negative control.

ATF3 in Ang II-induced HCFs, the effects of ATF3 knockdown on Ang II-induced HCFs were assessed. ATF3 knockdown significantly enhanced Ang II-induced HCF viability compared with that in cells transfected with the negative control (Fig. 3A). Cell migration was also demonstrated to be significantly increased by ATF3 knockdown compared with that in the si-NC group, and the protein expression levels of MMP-1 and MMP-2 were significantly potentiated in Ang II-induced HCFs transfected with si-ATF3 compared with those in the Ang II + si-NC group (Fig. 3B and C). Subsequently,  $\alpha$ -SMA protein expression was demonstrated to be increased following transfection with si-ATF3, compared with that in the Ang II + si-NC cells (Fig. 3D). ATF3 knockdown also significantly promoted the protein expression levels of CTGF, fibronectin, collagen I and collagen III in Ang II-induced HCFs compared with those in the Ang II + si-NC group (Fig. 3E).

*ATF3 promotes the transcriptional activation of Cyr61.* The potential mechanisms by which ATF3 regulated Ang II-induced

HCFs were evaluated. Compared with those in their corresponding negative controls, ATF3 overexpression significantly increased the mRNA and protein expression levels of Cyr61 in HCFs, whereas they were significantly decreased by ATF3 silencing (Fig. 4A and B). A binding site was predicted using the JASPAR database (Fig. 4C). The luciferase reporter assay demonstrated that the luciferase activity of the WT Cyr61 promoter was significantly increased by ATF3 overexpression compared with in the Oe-NC group, whereas no notable changes in the luciferase activity of the Mut Cyr61 promoter were observed (Fig. 4D). Furthermore, the ChIP assay verified that compared with the Oe-NC group, a significant increase was observed in the enrichment of Cyr61 promoter in ATF3 antibody in the Oe-ATF3 group, implying that ATF3 could bind to the predicted Cyr61 binding site (Fig. 4E).

*ATF3 affects Ang II-induced HCFs and TGF- $\beta$  signaling by regulating Cyr61.* To further explore the role of Cyr61

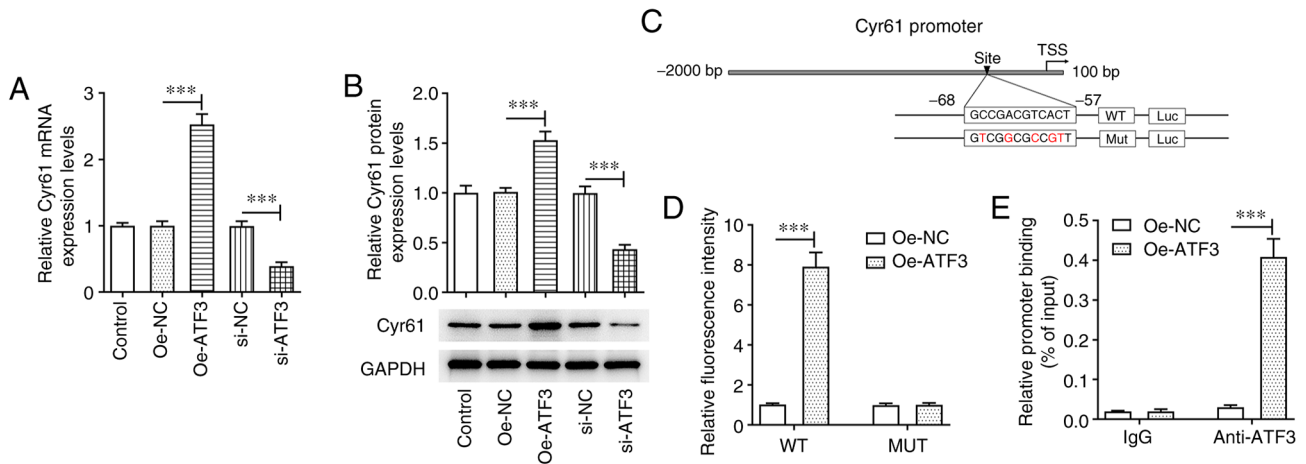


Figure 4. ATF3 promotes transcriptional activation of Cyr61 in human cardiac fibroblasts. (A) mRNA and (B) protein expression levels of Cyr61 were assessed using reverse transcription-quantitative PCR and western blotting, respectively. (C) The JASPAR database identified the binding site of ATF3 and Cyr61 promoter. (D) A luciferase reporter assay was used to assess the luciferase activity of the Cyr61 promoter. (E) A chromatin immunoprecipitation assay was performed to evaluate the binding of ATF3 to Cyr61. Data are presented as the mean  $\pm$  SD. \*\*\* $P$ <0.001. ATF3, activating transcription factor 3; Cyr61, cysteine-rich angiogenic protein 61; Oe, overexpression; NC, negative control; si, small interfering RNA; WT, wild-type; Mut, mutant; TSS, transcription start site.

in Ang II-induced HCFs following ATF3 manipulation, Cyr61 expression was knocked down by transfection with si-Cyr61-1/2. The transfection efficiency was assessed using RT-qPCR and western blotting. Since si-Cyr61-1 transfection resulted in superior transfection efficiency (Fig. 5A and B), si-Cyr61-1 was chosen for use in subsequent experiments and is referred to as si-Cyr61 thereafter. CCK-8 assay results demonstrated that Cyr61 knockdown increased the Oe-ATF3-reduced cell viability (Fig. 5C). Furthermore, ATF3 overexpression significantly suppressed cell migration, and markedly declined MMP-1 and MMP-2 expression in Ang II-treated HCFs, which was reversed by Cyr61 silencing (Fig. 5D and E).  $\alpha$ -SMA protein expression levels were reversed by Cyr61 silencing compared with the Oe-ATF3 group when assessed using immunofluorescence staining, and the protein expression levels of CTGF, fibronectin, collagen I and collagen III were elevated in Cyr61-silenced cells compared with those in the Ang II+Oe-ATF3 group (Fig. 5F and G). Furthermore, the protein expression levels of TGF- $\beta$ , p-Smad2/Smad2 and p-Smad3/Smad3 were significantly increased by stimulation with Ang II, and were in turn significantly reduced by ATF3 overexpression (Fig. 5H). However, Cyr61 knockdown significantly reversed the effects of ATF3 overexpression on the protein expression levels of these three aforementioned proteins.

## Discussion

During cardiac hypertrophy, the regulation of cardiac fibroblasts by Ang II and other factors results in excessive proliferation and the production of excessive quantities of fibrin, which leads to cardiac fibrosis and can further aggravate cardiac hypertrophy (26-28). Therefore, inhibition of the proliferation and fibrosis of cardiac fibroblasts may serve as a viable strategy for treating cardiac hypertrophy. The present study aimed to evaluate the therapeutic potential of ATF3

for alleviating cardiac viability and fibrosis in addition to assessing the potential molecular mechanism underlying its function using an *in vitro* model.

ATF3 is a stress response protein, the expression of which rapidly increases following stress stimulation by endogenous and exogenous factors, in order to regulate the expression of target genes (29). Li *et al* (30) reported that cardiac fibroblasts were the main cell type that express ATF3 in response to stimulation. ATF3 expression has been reported to be upregulated in Ang II- and aortic constriction-induced mouse myocardium, whereas ATF3 knockdown could worsen Ang II-induced cardiac fibrosis and hypertrophy (31). These findings suggested that ATF3 may serve an important regulatory role in myocardial fibrosis. In the present study, HCFs were stimulated with Ang II and it was demonstrated that Ang II treatment significantly increased the mRNA and protein expression levels of ATF3. ATF3 overexpression also exerted a significant inhibitory effect on Ang II-induced increases in HCF viability, migration and fibrosis. ATF3 expression was subsequently silenced and it was demonstrated that it mediated the opposite effects on Ang II-induced HCF viability, migration and fibrosis compared with ATF3 overexpression, which suggested a possible protective role for ATF3 against Ang II-induced stress in HCFs. These results were consistent with those of a previous study, which reported that reduced ATF3 expression may promote stress overload-induced cardiac hypertrophy, dysfunction and fibrosis (21).

It has previously been reported that ATF3 can transcriptionally upregulate Cyr61 expression in hepatocellular carcinoma (32). Cyr61, also known as cellular communication network factor (CCN)1, is a member of the CCN family of proteins that serves as an angiogenic factor (33). Previous studies have reported that Cyr61 expression is elevated during chronic heart failure and is associated with Ang (34-36). In the present study, a binding site of ATF3 on the Cyr61 promoter was predicted using the JASPAR database, which was verified experimentally using a combination of luciferase reporter

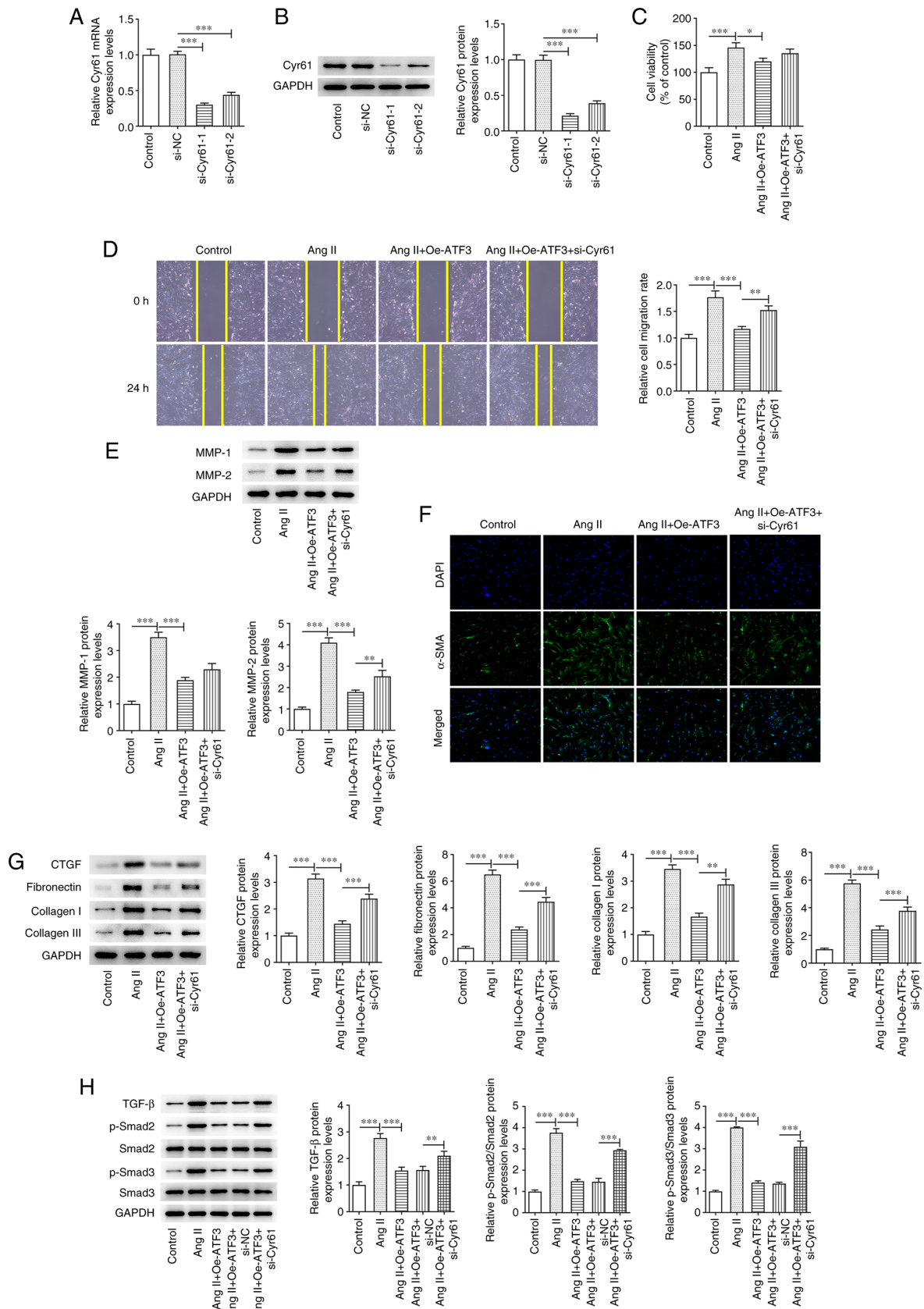


Figure 5. ATF3 regulates Ang II-induced development of cardiac fibroblasts and the TGF- $\beta$  signaling pathway through binding to Cyr61. (A) mRNA and (B) protein expression levels of Cyr61 were detected using reverse transcription-quantitative PCR and western blotting respectively. (C) Cell viability was evaluated using a Cell Counting Kit-8 assay. (D) Cell migration was evaluated using a wound healing assay (magnification,  $\times 100$ ). (E) Protein expression levels of MMP-1 and MMP-2 were semi-quantified using western blotting. (F) Immunofluorescence staining was performed to assess the protein expression levels of  $\alpha$ -SMA (magnification,  $\times 200$ ). Protein expression levels of (G) CTGF, fibronectin, collagen I and collagen III, and (H) TGF- $\beta$ , p-Smad2, p-Smad3, Smad2 and Smad3 were semi-quantified using western blotting. Data are presented as the mean  $\pm$  SD. \* $P < 0.05$ , \*\* $P < 0.01$ , \*\*\* $P < 0.001$ . ATF3, activating transcription factor 3; Ang II, angiotensin II;  $\alpha$ -SMA,  $\alpha$ -smooth muscle actin; Cyr61, cysteine-rich angiogenic protein 61; p, phosphorylated; CTGF, connective tissue growth factor; Oe, overexpression; NC, negative control; si, small interfering RNA.



and ChIP assays. You *et al* (37) reported that Cyr61/CCN1 expression was regulated by the cooperation of c-Jun/AP-1 and hypoxia inducible factor-1 $\alpha$  under hypoxic conditions in retinal vascular endothelial cells. Furthermore, Cyr61 has been reported to suppress myocardial fibrosis and improve cardiac function (38). The present study silenced Cyr61 expression in Ang II-induced HCFs and demonstrated that it significantly reversed the effects of ATF3 overexpression on cell viability, migration and fibrosis, which suggested that ATF3 regulated HCFs induced by Ang II via transcriptional activation of Cyr61.

Numerous studies have reported that Ang II can induce the proliferation of cardiac fibroblasts through multiple signaling pathways, including the TGF- $\beta$ /MAPK and TGF- $\beta$ /Smad signaling pathways (39,40). It has previously been reported that the CCN protein family can moderate the production of growth factors and cytokine signaling (41). Borkham-Kamphorst *et al* (42) reported that CCN1 exerted anti-fibrotic effects through the induction of reactive oxygen species, which in turn attenuated TGF- $\beta$  signaling by scavenging the TGF- $\beta$  ligand. In the present study, significant increases in the protein expression levels of TGF- $\beta$ , p-Smad2/Smad2 and p-Smad3/Smad3 were detected in Ang II-induced HCFs. ATF3 overexpression significantly reversed this increase in the expression levels of these proteins. However, Cyr61 knockdown significantly negated the effects induced by ATF3 overexpression on the increased levels of TGF- $\beta$ , p-Smad2 and p-Smad3. These results suggested that the TGF- $\beta$ /Smad pathway may be involved in the modulation of ATF3/Cyr61-mediated viability and fibrosis of HCFs. Notably, there were several limitations in the present study. Only *in vitro* experiments were performed and further *in vivo* experiments are required to confirm the results in future studies. Furthermore, the potential mechanisms and key pathways require elucidation in future studies.

In conclusion, the present study demonstrated that ATF3 overexpression could suppress the viability, migration and fibrosis of HCFs through the transcriptional activation of Cyr61. These findings may provide novel insights into anti-viability and anti-fibrosis strategies for the treatment of cardiac hypertrophy.

## Acknowledgements

Not applicable.

## Funding

The present study was supported by the Scientific Research and Cultivation Project of Meizhou People's Hospital, China (grant no. PY-C20210026).

## Availability of data and materials

The datasets used and/or analyzed during the current study are available from the corresponding author on reasonable request.

## Authors' contributions

YZ, HW, HL and CH designed the study and performed the experiments. YZ, HW, HL and YL wrote the manuscript and

analyzed the data. YZ supervised the experiments and revised the manuscript. YZ and HW confirm the authenticity of all the raw data. All authors read and approved the final manuscript.

## Ethics approval and consent to participate

Ethics approval for the use of human cardiac fibroblasts was waived by Meizhou People's Hospital.

## Patient consent for publication

Not applicable.

## Competing interests

The authors declare that they have no competing interests.

## References

1. Nakamura M and Sadoshima J: Mechanisms of physiological and pathological cardiac hypertrophy. *Nat Rev Cardiol* 15: 387-407, 2018.
2. Shimizu I and Minamino T: Physiological and pathological cardiac hypertrophy. *J Mol Cell Cardiol* 97: 245-262, 2016.
3. Zhu L, Li C, Liu Q, Xu W and Zhou X: Molecular biomarkers in cardiac hypertrophy. *J Cell Mol Med* 23: 1671-1677, 2019.
4. Gallo S, Vitacolonna A, Bonzano A, Comoglio P and Crepaldi T: ERK: A key player in the pathophysiology of cardiac hypertrophy. *Int J Mol Sci* 20: 2164, 2019.
5. Wang L, Wang J, Li G and Xiao J: Non-coding RNAs in physiological cardiac hypertrophy. *Adv Exp Med Biol* 1229: 149-161, 2020.
6. Tham YK, Bernardo BC, Ooi JY, Weeks KL and McMullen JR: Pathophysiology of cardiac hypertrophy and heart failure: Signaling pathways and novel therapeutic targets. *Arch Toxicol* 89: 1401-1438, 2015.
7. Bisping E, Wakula P, Poteser M and Heinzel FR: Targeting cardiac hypertrophy: Toward a causal heart failure therapy. *J Cardiovasc Pharmacol* 64: 293-305, 2014.
8. Hou J and Kang YJ: Regression of pathological cardiac hypertrophy: Signaling pathways and therapeutic targets. *Pharmacol Ther* 135: 337-354, 2012.
9. Persengiev SP and Green MR: The role of ATF/CREB family members in cell growth, survival and apoptosis. *Apoptosis* 8: 225-228, 2003.
10. Zabala V, Boylan JM, Thevenot P, Frank A, Senthooor D, Iyengar V, Kim H, Cohen A, Gruppiso PA and Sanders JA: Transcriptional changes during hepatic ischemia-reperfusion in the rat. *PLoS One* 14: e0227038, 2019.
11. Shi Z, Zhang K, Chen T, Zhang Y, Du X, Zhao Y, Shao S, Zheng L, Han T and Hong W: Transcriptional factor ATF3 promotes liver fibrosis via activating hepatic stellate cells. *Cell Death Dis* 11: 1066, 2020.
12. Qian L, Zhao Y, Guo L, Li S and Wu X: Activating transcription factor 3 (ATF3) protects against lipopolysaccharide-induced acute lung injury via inhibiting the expression of TL1A. *J Cell Physiol* 232: 3727-3734, 2017.
13. Chen SC, Liu YC, Shyu KG and Wang DL: Acute hypoxia to endothelial cells induces activating transcription factor 3 (ATF3) expression that is mediated via nitric oxide. *Atherosclerosis* 201: 281-288, 2008.
14. Bueno M, Brands J, Voltz L, Fiedler K, Mays B, St Croix C, Sembrat J, Mallampalli RK, Rojas M and Mora AL: ATF3 represses PINK1 gene transcription in lung epithelial cells to control mitochondrial homeostasis. *Aging Cell* 17: e12720, 2018.
15. Zhao W, Sun M, Li S, Chen Z and Geng D: Transcription factor ATF3 mediates the radioresistance of breast cancer. *J Cell Mol Med* 22: 4664-4675, 2018.
16. Ku HC and Cheng CF: Master regulator activating transcription factor 3 (ATF3) in metabolic homeostasis and cancer. *Front Endocrinol (Lausanne)* 11: 556, 2020.
17. Kumar M, Majumder D, Mal S, Chakraborty S, Gupta P, Jana K, Gupta UD, Ghosh Z, Kundu M and Basu J: Activating transcription factor 3 modulates the macrophage immune response to *Mycobacterium tuberculosis* infection via reciprocal regulation of inflammatory genes and lipid body formation. *Cell Microbiol* 22: e13142, 2020.

18. Zhou H, Li N, Yuan Y, Jin YG, Guo H, Deng W and Tang QZ: Activating transcription factor 3 in cardiovascular diseases: A potential therapeutic target. *Basic Res Cardiol* 113: 37, 2018.
19. Qin W, Yang H, Liu G, Bai R, Bian Y, Yang Z and Xiao C: Activating transcription factor 3 is a potential target and a new biomarker for the prognosis of atherosclerosis. *Hum Cell* 34: 49-59, 2021.
20. Li YL, Hao WJ, Chen BY, Chen J and Li GQ: Cardiac fibroblast-specific activating transcription factor 3 promotes myocardial repair after myocardial infarction. *Chin Med J (Engl)* 131: 2302-2309, 2018.
21. Zhou H, Shen DF, Bian ZY, Zong J, Deng W, Zhang Y, Guo YY, Li H and Tang QZ: Activating transcription factor 3 deficiency promotes cardiac hypertrophy, dysfunction, and fibrosis induced by pressure overload. *PLoS One* 6: e26744, 2011.
22. Zhou Y, Xie Y, Li T, Zhang P, Chen T, Fan Z and Tan X: P21-activated kinase 1 mediates angiotensin II-induced differentiation of human atrial fibroblasts via the JNK/c-Jun pathway. *Mol Med Rep* 23: 207, 2021.
23. Gwathmey TM, Pendergrass KD, Reid SD, Rose JC, Diz DI and Chappell MC: Angiotensin-(1-7)-angiotensin-converting enzyme 2 attenuates reactive oxygen species formation to angiotensin II within the cell nucleus. *Hypertension* 55: 166-171, 2010.
24. Yang LL, Li DY, Zhang YB, Zhu MY, Chen D and Xu TD: Salvianolic acid A inhibits angiotensin II-induced proliferation of human umbilical vein endothelial cells by attenuating the production of ROS. *Acta Pharmacol Sin* 33: 41-48, 2012.
25. Livak KJ and Schmittgen TD: Analysis of relative gene expression data using real-time quantitative PCR and the 2(-Delta Delta C (T)) method. *Methods* 25: 402-408, 2001.
26. Zhai CG, Xu YY, Tie YY, Zhang Y, Chen WQ, Ji XP, Mao Y, Qiao L, Cheng J, Xu QB and Zhang C: DKK3 overexpression attenuates cardiac hypertrophy and fibrosis in an angiotensin-perfused animal model by regulating the ADAM17/ACE2 and GSK-3 $\beta$ /catenin pathways. *J Mol Cell Cardiol* 114: 243-252, 2018.
27. Sheng R, Gu ZL, Xie ML, Zhou WX and Guo CY: EGCG inhibits proliferation of cardiac fibroblasts in rats with cardiac hypertrophy. *Planta Med* 75: 113-120, 2009.
28. Ji Y, Qiu M, Shen Y, Gao L, Wang Y, Sun W, Li X, Lu Y and Kong X: MicroRNA-327 regulates cardiac hypertrophy and fibrosis induced by pressure overload. *Int J Mol Med* 41: 1909-1916, 2018.
29. Nyunt T, Britton M, Wanichthanarak K, Budamagunta M, Voss JC, Wilson DW, Rutledge JC and Aung HH: Mitochondrial oxidative stress-induced transcript variants of ATF3 mediate lipotoxic brain microvascular injury. *Free Radic Biol Med* 143: 25-46, 2019.
30. Li Y, Li Z, Zhang C, Li P, Wu Y, Wang C, Bond Lau W, Ma XL and Du J: Cardiac fibroblast-specific activating transcription factor 3 protects against heart failure by suppressing MAP2K3-p38 signaling. *Circulation* 135: 2041-2057, 2017.
31. Pan J, Xu Z, Guo G, Xu C, Song Z, Li K, Zhong K and Wang D: Circ\_nuclear factor I X (circNfix) attenuates pressure overload-induced cardiac hypertrophy via regulating miR-145-5p/ATF3 axis. *Bioengineered* 12: 5373-5385, 2021.
32. Chen C, Ge C, Liu Z, Li L, Zhao F, Tian H, Chen T, Li H, Yao M and Li J: ATF3 inhibits the tumorigenesis and progression of hepatocellular carcinoma cells via upregulation of CYR61 expression. *J Exp Clin Cancer Res* 37: 263, 2018.
33. Chaqour B: Regulating the regulators of angiogenesis by CCN1 and taking it up a Notch. *J Cell Commun Signal* 10: 259-261, 2016.
34. Bonda TA, Kamiński KA, Dziemidowicz M, Litvinovich S, Kożuch M, Hirnle T, Dmitruk I, Chyczewski L and Winnicka MM: Atrial expression of the CCN1 and CCN2 proteins in chronic heart failure. *Folia Histochem Cytobiol* 50: 99-103, 2012.
35. Wang J, Fu D, Senouthai S, Jiang Y, Hu R and You Y: Identification of the transcriptional networks and the involvement in Angiotensin II-induced injury after CRISPR/Cas9-mediated knockdown of Cyr61 in HEK293T cells. *Mediators Inflamm* 2019: 8697257, 2019.
36. Hilfiker A, Hilfiker-Kleiner D, Fuchs M, Kaminski K, Lichtenberg A, Rothkötter HJ, Schieffer B and Drexler H: Expression of CYR61, an angiogenic immediate early gene, in arteriosclerosis and its regulation by angiotensin II. *Circulation* 106: 254-260, 2002.
37. You JJ, Yang CM, Chen MS and Yang CH: Regulation of Cyr61/CCN1 expression by hypoxia through cooperation of c-Jun/AP-1 and HIF-1 $\alpha$  in retinal vascular endothelial cells. *Exp Eye Res* 91: 825-836, 2010.
38. Meyer K, Hodwin B, Ramanujam D, Engelhardt S and Sarikas A: Essential role for premature senescence of myofibroblasts in myocardial fibrosis. *J Am Coll Cardiol* 67: 2018-2028, 2016.
39. Li L, Fan D, Wang C, Wang JY, Cui XB, Wu D, Zhou Y and Wu LL: Angiotensin II increases periostin expression via Ras/p38 MAPK/CREB and ERK1/2/TGF- $\beta$ 1 pathways in cardiac fibroblasts. *Cardiovasc Res* 91: 80-89, 2011.
40. Wu X, Liu Y, An J, Li J, Lv W, Geng S and Zhang Y: Piperlongumine inhibits angiotensin II-induced extracellular matrix expression in cardiac fibroblasts. *J Cell Biochem* 119: 10358-10364, 2018.
41. Leask A and Abraham DJ: All in the CCN family: Essential matricellular signaling modulators emerge from the bunker. *J Cell Sci* 119: 4803-4810, 2006.
42. Borkham-Kamphorst E, Schaffrath C, Van de Leur E, Haas U, Tihaa L, Meurer SK, Nevzorova YA, Liedtke C and Weiskirchen R: The anti-fibrotic effects of CCN1/CYR61 in primary portal myofibroblasts are mediated through induction of reactive oxygen species resulting in cellular senescence, apoptosis and attenuated TGF- $\beta$  signaling. *Biochim Biophys Acta* 1843: 902-914, 2014.



This work is licensed under a Creative Commons Attribution-NonCommercial-NoDerivatives 4.0 International (CC BY-NC-ND 4.0) License.